A parsimonious water budget model for Canadian agricultural conditions

Martel, Myra; Glenn, Aaron; Wilson, Henry; Danielescu, Serban; Kröbel, Roland; Smith, Ward; McConkey, Brian; Guest, Geoffrey; Janzen, Henry

Publisher's version / Version de l'éditeur:
https://doi.org/10.1016/j.ejrh.2021.100846
Journal of Hydrology: Regional Studies, 36, C, 2021-06-14

Journal of Hydrology: Regional Studies 36 (2021) 100846

Contents lists available at ScienceDirect

Journal of Hydrology: Regional Studies

journal homepage: www.elsevier.com/locate/ejrh

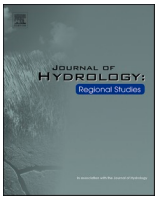

A parsimonious water budget model for Canadian agricultural conditions

Myra Martel [a,b], Aaron Glenn [c], Henry Wilson [c], Serban Danielescu [d], Roland Kröbel [a,*], Ward Smith [e], Brian McConkey [f], Geoffrey Guest [g], Henry Janzen [a]

[a] Agriculture and Agri-Food Canada (AAFC), Lethbridge Research and Development Centre, Lethbridge, Alberta, Canada
[b] Chemical and Biological Engineering, University of Saskatchewan, Saskatoon, Saskatchewan, Canada
[c] AAFC, Brandon Research and Development Centre, Brandon, Manitoba, Canada
[d] AAFC and Environment and Climate Change Canada (ECCC), Fredericton Research and Development Centre, Fredericton, New Brunswick, Canada
[e] AAFC, Ottawa Research and Development Centre, Carling Ave., Ottawa, Canada
[f] AAFC, Swift Current Research and Development Centre, Swift Current, Canada
[g] National Research Council Canada, Ottawa, Canada

ARTICLE INFO

Keywords:
Agri-hydrological model
Deep percolation
Evapotranspiration
Runoff
Soil moisture

ABSTRACT

Study region: This study used data collected from three cropland sites (two in Manitoba and one in Prince Edward Island) in Canada.
Study focus: In efforts to accurately describe the water dynamics in agricultural soils, most of the agri-hydrological models developed are highly complex, such that they require detailed input data, of which most of them are not always measured or otherwise readily available. However, the comprehensive and complex representations of the processes may not be justified when data is scarce. Thus, this study developed a soil water budget model that could describe the movement of water through Canadian agricultural soils using a few parameters only. The model was developed by selecting algorithms from various existing models, whose data requirements are readily available in literature and public Canadian databases.
New hydrological insights: The model developed in this study can simulate evapotranspiration, runoff, deep percolation, and soil moisture content for various seasons (i.e., growing, non-growing/dormant, and pre-planting/post-harvest) with minimum data requirement, which addresses the limited availability of data in the country for crop and hydrological modeling. Moreover, the model is simple and easy to use, and can work without calibration. It was tested using three site-specific datasets, and results show that despite its simplicity, its overall performance was comparable with those of other agricultural models that use cascade flow framework for hydrology.

1. Introduction

Soil water has a wide range of effects on crop growth and yield (Raes et al., 2006; Aina et al., 2007; Bennett and Harms, 2011) and affects the rate and movement of water within agricultural landscapes; hence, it becomes an important consideration in the implementation of various cropping systems and influences many agricultural management decisions. For instance, the timing and

* Corresponding author.
E-mail address: roland.kroebel@canada.ca (R. Kröbel).

https://doi.org/10.1016/j.ejrh.2021.100846
Received 20 February 2020; Received in revised form 14 May 2021; Accepted 7 June 2021
Available online 14 June 2021

application rate of fertilizer and irrigation water and the design and operation of tile drainage systems depend on the water content of the soil profile. Further, the increasing concern regarding the impacts of agriculture on water resources, both from quality and quantity perspectives, intensifies a need to have an accurate accounting of water budgets within agricultural landscapes. Measuring and monitoring storage and movement of water in soils are, therefore, crucial for developing and achieving sustainable agricultural management systems; however, these measurements are generally costly as they have to be continually carried out to observe responses to climate and soil properties. Thus, when field measurements are not available, soil water balance simulation is often used (Perez-Sanchez et al., 2019).

Soil water balance simulation applies the principle of mass balance, where the change of moisture content in a soil reservoir (e.g., root zone) is determined through additions and losses of water. It generally simulates processes such as infiltration of rain or irrigation water, runoff of water exceeding soil infiltration rate, redistribution of infiltrated water within the root zone, evapotranspiration of water from plants and soil surfaces, and percolation of water out of the root zone (deep drainage).

A number of soil water balance simulation models with varying degrees of complexity and data requirements are available for various hydrological applications (ranging from simple volume balance models to sophisticated dynamic models). Dynamic and semi-dynamic models [e.g., Hydrus (PC-Progress, 2019) and root zone water quality model (RZWQM; USDA, 2020)] describe saturated-unsaturated water flow in soil through more detailed process-based transport phenomena expressed as differential equations, such as the Richards' equation; thus, they require more specific data, such as unsaturated soil hydraulic properties, which are difficult to measure and rarely available in most soil databases. Moreover, analytical solution to the Richards' equation is limited to a few simple cases only due to the high nonlinear dependence of hydraulic conductivity and diffusivity on moisture content (Islam et al., 2017). Even with numerical approaches, solution to the Richards' equation still remains challenging despite numerous efforts (Farthing and Ogden, 2017; Zhu et al., 2018: Gao et al., 2019). Mass balance and non-convergence problems sometimes exist in applying this equation for water flow as it assumes a consistent hydraulic gradient, which is often not the case in heterogeneous agricultural soil profiles (Beven and Germann, 2013).

In contrast, volume balance or budget models follow a semi-empirical approach to avoid complicated differential equations in describing water dynamics. For that purpose, the concept of water holding capacity (defined by saturation, field capacity, and wilting point) of distinct soil layers is employed. The soil layers are represented as 'tipping buckets' (each having a specified capacity to hold water). The water in the upper layer moves down to the lower layer when the upper layer exceeds its water holding capacity (cascade approach). However, despite the general simplicity of the budgeting approach, a number of models that apply this concept [e.g., soil and water assessment tool (SWAT; Texas A&M University, 2021), AquaCrop (Food and Agriculture Organization of the United Nations (FAO), 2021), simulateur multidisciplinaire pour les cultures standard (STICS; National Research Institute for Agriculture, Food and Environment (National Research Institute for Agriculture, Food and Environment (INRAE), 2020), and denitrification and decomposition model (DNDC; University of New Hampshire, 2021)] also require detailed input data for specific algorithms that are not always measured or otherwise readily available, such as canopy cover, leaf area index, and above ground biomass. As these models also simulate other ecological processes (e.g., carbon and nitrogen cycling), they require inputs that may not be necessary for quick and simple water budget estimates. Moreover, these models often need to be calibrated when applied in regions with different agricultural and environmental conditions (Malago et al., 2015; Faramarzi et al., 2017; Smith et al., 2020). When data is scarce, calibration becomes challenging, particularly with complex models, which typically involve large number of parameters (Hishinuma et al., 2014). Although there are a couple of models originally developed for Canadian agricultural conditions, they are also facing some limitations. For instance, the versatile soil moisture budget (VSMB) model, which was originally developed by Baier and Robertson (1966), is not relatively simple to implement, particularly with its empirically-derived drying curves. Further, it does not have crop-specific root extraction coefficients, except for those that were validated in recent studies (Akinremi et al., 1996; Hayashi et al., 2010; Hayashi et al., 2012), and requires site-specific calibration before implementation. In addition, the Alberta Irrigation Management Model (AIMM; Alberta Agriculture and Forestry, 2020), though relatively straightforward, does not estimate runoff, as it was mainly designed for irrigation scheduling.

Thus, the objective of this study was to develop a water budget model for simulating movement of water within Canadian agricultural landscapes with the following criteria: (1) the model can simulate main water fluxes (i.e., evapotranspiration, surface runoff, deep percolation, and soil water storage) with a few parameters only (parsimonious) to address the limited availability of data in the country for crop and hydrological modeling, (2) the required data can be easily obtained from literature and Canadian databases [e.g., National Soil Database (NSDB) and climate data from Environment and Climate Change Canada (ECCC)], and (3) the model is simple and easy to use (can work without calibration). The model was developed by selecting and combining algorithms from various existing models that satisfy the abovementioned criteria. This paper presents the conceptual framework, sensitivity and uncertainty analyses, and testing of the model.

2. Methods

2.1. Model description

2.1.1. Model simulation for various seasons

The model, which is intended to be incorporated into the Holos model (Agriculture and Agri-Food Canada (AAFC), 2020) of Agriculture and Agri-Food Canada as its hydrological component, simulates soil moisture content and movement of water across agricultural landscapes during different stages of plant growth, as well as during off-season (pre-planting and post-harvest) and non-growing and dormant periods (Fig. 1). Growing period spans from planting to harvest (which varies depending on crop, location,

and climate). Non-growing and dormant periods start when daily minimum air temperatures are 0 °C or below for five consecutive days after October 31st and end when this temperature requirement is no longer satisfied any day after March 31st. Although non-growing and dormant periods are theoretically similar in the context of temperature requirement, dormant, in the model, particularly refers to the case when the field is planted with a crop (e.g., winter wheat) that stops growing during winter, while non-growing period applies when the field is not planted with any crop. The two cases have to be distinguished as they use different surface coefficients. The period outside growing, non-growing, and dormant periods is considered off-season. Other events can also be simulated by choosing any of the aforementioned events/periods that closely describe them. For instance, fallow can be simulated as off-season.

2.1.2. Soil profile and soil water storage

In the model, the entire soil profile is divided into four layers. The partitioning of the soil profile into four layers, as well as the depth of each layer, is user-defined. The only requisite is that the upper most layer (Layer 1) should not be less than 10 cm, as explained in the next paragraph below. There is flexibility in the model to allow users to partition the soil profile into four layers the way it fits for their study. For instance, in simulating deep-rooted crops, such as alfalfa, which can have a maximum rooting depth of 2 m, the A, B, and C main soil horizons indicated in the Canadian System of Soil Classification could be assigned to Layers 1, 2, and 3, respectively. As the soil information provided in the National Soil Database (Agriculture and Agri-Food Canada (AAFC), 2021) is generally available for depths of up to 1.0–1.2 m only, the C horizon could be extended to compensate for the remaining portion of the rooting depth. The extended C horizon is designated as Layer 4, and assumes the properties of the C horizon. This particular case was the main consideration for the four-layer partitioning. In cases where the maximum rooting depth is up to the B horizon only, such as with shallow-rooted crops, the soil profile could be partitioned this way: A horizon for Layer 1, and three partitions of the B horizon for Layers 2, 3, and 4. Another way to partition the soil profile is shown in Fig. 2. Here, the A and B horizons are assigned to Layers 1 and 2, respectively. Part of the C horizon that could be penetrated with roots is designated as Layer 3, while the remaining portion of the C horizon (below the maximum rooting depth) is designated as Layer 4. With this flexibility, it is possible to simulate soil moisture content involving shallow- and deep-rooted crops. It is also possible to simulate soil moisture content up to the depth of the ground water table, provided there is no interceptive layer (e.g., clay pan, rock) that prevents further downward movement of water. It should be noted that the number of ways the soil profile can be partitioned into four layers is not limited to the examples given above.

Through an internal process, the model classifies each of the soil layers as either surface, root, or below root zones (Fig. 2) (Layer 1 is automatically classified as surface zone). In each of these zones, different mass balance equation (all model equations are found in Appendix A in the Supplementary Material) is implemented. Equation (A.1) describes the water that flows in and out of the surface zone. Equation (A.2) accounts for the water flowing through the root zone, while Eq. (A.3) describes the water moving out of the root zone (below root zone). These equations are adapted from the pesticide root zone model (PRZM; Suarez, 2005; Joint Research Centre, 2021). The model classifies the soil layers into these three zones as the soil water mass balances are calculated based on the depths of these zones, which change with root dynamics, except the surface zone which is fixed throughout simulation. The surface zone corresponds to the uppermost soil layer (i.e., Layer 1); hence, its depth is fixed throughout simulation. As mentioned earlier, the depth of Layer 1 should not be less than 10 cm to have sufficient depth to account for evaporation and runoff/infiltration. The depths of the root and below root zones vary in correspondence to the root dynamics (i.e., root zone depth increases while below root zone depth decreases as roots expand).

2.1.3. Evapotranspiration

Evapotranspiration (ET) is the loss of water from a vegetated surface through the combined processes of soil evaporation and plant transpiration. In the beginning of the season when the crop is small and the soil surface is exposed, evaporation is the dominant process; however, once the crop has fully grown and completely covers the soil, transpiration becomes the governing process (Allen et al., 1998). As both processes occur simultaneously, it is difficult to estimate the two separately and accurately without utilizing a phenological crop growth model that provides a reliable transpiration estimate. Such addition would require parameters that are sometimes not measurable, or generally available only from very specific experiments (e.g., photosynthetic rate or radiation use efficiency, photoperiod, canopy cover, leaf area expansion). It would also require algorithms that govern above-ground biomass accumulation and growth stage initialization (e.g., solar radiation intensity, temperature triggers) (Wang and Engel, 1998; Wang et al., 2002). Most of the models that adopt this approach are crop models or, at least, have a crop growth component [e.g., AquaCrop,

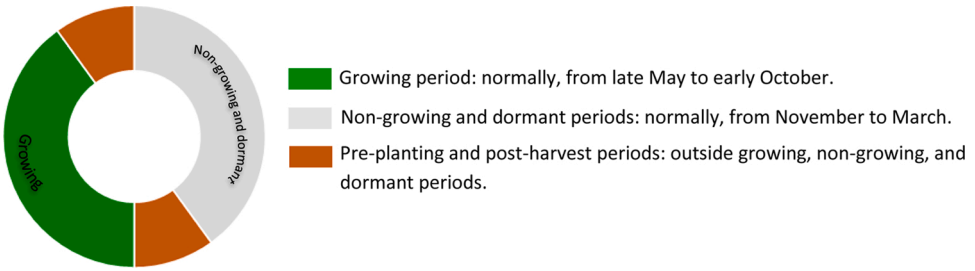

Fig. 1. Diagram illustrating the various periods simulated in the model.

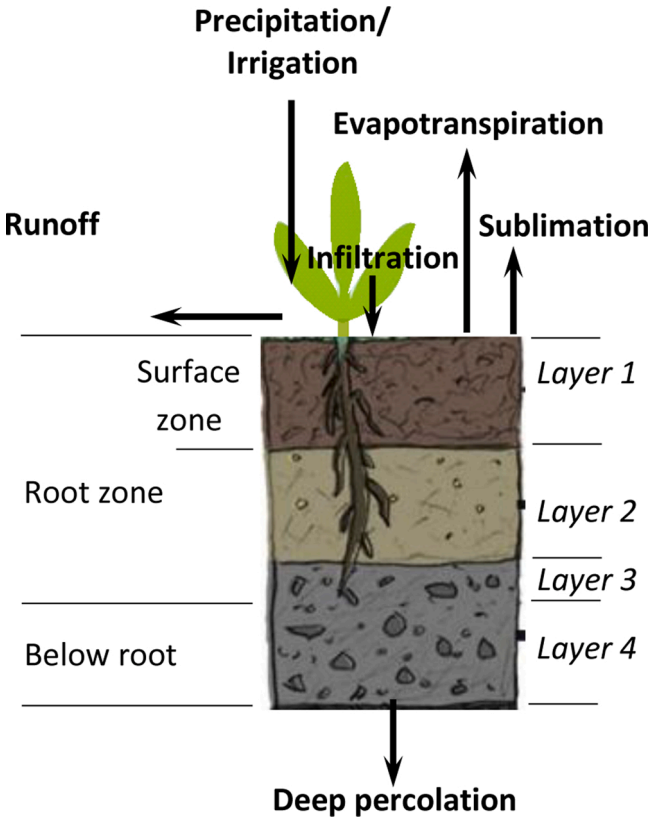

Fig. 2. Diagram of a soil profile acting as a reservoir showing various water fluxes that affect its moisture content. This diagram also shows one of the ways the soil profile can be partitioned into four layers.

decision support system for agrotechnology transfer (DSSAT), SWAT, environmental policy integrated climate (EPIC)], or models that deal with nutrient cycling/uptake (e.g., PRZM), where a more accurate estimate for transpiration is necessary. As the primary intended use of the current model is for generating localized soil water balance estimates with minimum input requirements, calculation of evapotranspiration from combined evaporation and transpiration has been deemed sufficient to achieve the objective of this study.

Depending on available climate data, the model can estimate reference evapotranspiration using the FAO56 Penman-Monteith equation (Allen et al., 1998) or potential evapotranspiration using the Makkink (Makkink, 1957) or Hargreaves-Samani (Hargreaves and Samani, 1985) equations (see Appendix B in the Supplementary Material for the descriptions of these equations; in this paper, the acronym ET_R is used to refer to both reference and potential evapotranspiration). Martel et al. (2018) found that the Makkink and Hargreaves-Samani equations had comparable performance with the FAO56 Penman-Monteith equation using the meteorological data collected in the Canadian prairies. With these options, the ET_R can be estimated even with only air temperature data. The model adopts the crop coefficient approach [Eq. (A.4)] presented in FAO56 (Allen et al., 1998) for the estimation of actual crop evapotranspiration (ET_C). The crop coefficients (K_C) used in the model (listed in Appendix C), which are available for more than 50 crops, are fourth order functions of growing-degree-day (GDD); thus, their values vary over the growing period. Most of these coefficients were adopted from the AIMM model (Alberta Agriculture and Forestry, 2020). As the FAO56 Penman-Monteith equation uses grass-based K_C, these alfalfa-based K_C are converted to grass-based using Eq. (A.5) (Allen et al., 1998). The parameter K_R in Eq. (A.4) accounts for the effects of water availability in the root zone on ET_C as described in Eq. (A.6). Values for K_R could range from 0 (maximum water stress) to 1 (minimum or no water stress). The default minimum value for K_R in the model was set at 0.1, similar to what is applied in AIMM (Alberta Agriculture and Forestry, 2020); however, the user can always modify this value depending on what seems more suitable for the location under study. Evapotranspiration is removed from the entire root zone (including the surface zone). An in-depth discussion on the calculation of ET can be found in Martel et al. (2018). The model does not account for canopy interception. Due to the available GDD-based K_C, it can be applied only to monoculture system, except for barley silage underseeded in alfalfa. The K_C database is updated once new GDD-based K_C are developed.

2.1.4. Root expansion and extraction

The model simulates linear root expansion from minimum to maximum effective root depth. The minimum effective root depth (depth at the time of planting) is user defined; its default value was set at 0.2 m, which was adopted from the AquaCrop model (Raes et al., 2012). The maximum root depth is attained when K_C curve reaches its maximum. Once the maximum root depth is attained, it

remains constant until harvest. Planting and harvest dates are inputs to the model.

The active root zone is divided into four sections of equal vertical thickness. Each of these sections corresponds to a user defined root distribution, which determines the depth distribution of water extraction. The default values used in the model for root distribution are 40 %, 30 %, 20 %, and 10 % (Raes et al., 2012), which means that 40 % of the roots are found in the upper most quarter of the root zone, 30 % in the second lower quarter, 20 % in the third lower quarter, and 10 % in the bottom quarter. The rate at which water (as ET_C) is removed from each quarter follows the same proportion, which means that for the default values given above, 40 % of the total ET_C is removed from the upper most quarter, 30 % in the second lower quarter, and so on. If enough water is not available in a certain quarter, the demand is transferred to the next lower quarter at the minimum amount (i.e., at $K_R = 0.1$).

2.1.5. Evaporation during off-season

For the off-season (pre-planting and post-harvest) period, the model accounts only for evaporation from bare soil surface or reduced evaporation under crop residues (E_{OS}) in Layer 1. The approach applied for growing season [Eq. (A.4)] is used to estimate E_{OS}. A surface coefficient, K_{OS}, described in Eq. (A.7) (Snyder et al., 2007), which was derived for bare wet soil, is employed in lieu of K_C. A correction factor K_{R1} [similar to the one described in Eq. (A.6)] was also introduced to account for water availability in Layer 1. If the surface is under crop residues, the amount of E_{OS} is adjusted to account for the decrease in evaporation; a 5 % reduction for every 10 % of soil surface that is covered with residues is used, as suggested by Allen et al. (1998).

Weeds and volunteers (i.e., spontaneous plants that are not planted deliberately) during off-season (particularly for no-till and organic systems) could also affect the amount of E_{OS}; thus, for this condition, E_{OS} is adjusted to account for the water consumed by weeds and volunteers. The K_C value assigned for weeds/volunteers is 0.15 (adapted from Allen et al., 1998).

2.1.6. Sublimation and evaporation during non-growing and dormant periods

The model simulates evaporation from soil and sublimation from snow cover during non-growing and dormant periods (E_{NG}) in a way similar to estimating ET_C for growing season [Eq. (A.4)]; however, a surface coefficient (K_{NG}) was used in lieu of K_C. Although the ET_R equations were developed for vegetated surfaces or for growing period, they were used to estimate water losses during non-growing and dormant periods (Hay and Irmak, 2009). The value for K_{NG} used in the model is 0.44, adopted from a study conducted in a corn field in Nebraska during non-growing period with normal, wet, and dry seasons, including periods of snow cover (Hay and Irmak, 2009). This value is within the range (0.25–0.50) cited by Allen et al. (1998) for surface coefficients during non-growing and dormant periods. It should be noted that the user can override all crop and surface coefficients employed in the model if more suitable values are available.

If the soil surface is frozen ($T_{SS} \leq 0$ °C), the amount of sublimation is limited by the amount of snow cover stored as snow water equivalent (SWE). If E_{NG} is greater than SWE, the remainder of E_{NG} is taken from the soil surface layer; however, this is allowed only if $T_{SS} > 0$ °C and the soil moisture content of the surface layer is greater than 50 % of its wilting point.

2.1.7. Snowmelt

Precipitation is assumed to occur as rain if the daily mean temperature (T_m) is greater than or equal to 1.5 °C (Scheider et al., 1983), and snow if otherwise. Snow is accumulated in snowpack as SWE, and melting occurs when $T_m \geq 1.5$ °C. The amount of snowmelt is estimated using the empirical equations [Eqs. (A.8a and A.8b)] derived by Scheider et al. (1983) for Ontario conditions based on air mean temperature. Equation (A.8a) is used for dry weather condition, while Eq. (A.8b) is applied when there is rainfall as rain enhances melting of snow. The amount of snowmelt is limited by the amount of SWE in the snowpack [see Eqs. (A.8a and A.8b)]. Melted snow is treated as rainfall when estimating runoff and infiltration.

2.1.8. Surface runoff and infiltration

The model estimates surface runoff using the Natural Resources Conservation Service curve number (NRCS-CN) method [United States Department of Agriculture (United States Department of Agriculture (USDA), 2021)]. The runoff equation was modified to include both rain and snowmelt as inputs [Eqs. (A.9a and A.9b)]. The water that infiltrates into the soil is the difference between rain (plus snowmelt) and runoff [Eq. (A.17)]. However, the actual infiltration is limited by the saturation of Layer 1; thus, if the amount exceeds the saturation of Layer 1, the excess will be added to the amount of runoff estimated from Eq. (A.9a).

The model assumes that infiltration does not occur when soil surface is frozen ($T_{SS} \leq 0$ °C); thus, when this happens, any snowmelt or rainfall is considered surface runoff. Soil surface temperature (T_{SS}) is estimated using the equation [Eq. (A.18)] used by Akinremi et al. (1996) and Hayashi et al. (2012). It should be noted that the model does not account for land slope, ponding, runon, and subsurface drain.

2.1.9. Percolation

Percolation is simulated in the model based on a 'tipping bucket' approach, where water from the upper most layer percolates down to the next lower layer when field capacity is exceeded, with the process continuing down to the next succeeding soil layers until either all the percolating water is used up or all soil layers are brought to field capacity. The water that exceeds the field capacity of the lowest layer drains out of the soil profile (deep percolation) and recharges the ground water table, thus, considered lost from the soil profile. Upward water flow or capillary rise is not simulated in the model. Each soil layer can only take water up to its saturation and water can only percolate to the lower layer if the water content of the upper layer exceeds field capacity and that of the lower layer is below saturation. Percolating water (or part of it) from the upper layer that exceeds saturation of the lower layer will remain in the upper layer until it is used up or until the moisture content of the lower layer becomes less than saturation. The volume of water that

percolates from one layer to the underlying layer is calculated using the algorithm employed in the SWAT model [Eq. (A.20)] (Neitsch et al., 2011). Equation (A.22) shows that the time water percolates through soil layers depends mainly on the hydraulic properties of the soil. The model assumes no movement of water into and within the soil profile when soil surface is frozen. Further, it does not simulate soil freeze/thaw dynamics or perched water table conditions.

2.2. Model input requirements and outputs

The input parameters required to calculate the various water budget components discussed earlier include site location, soil and crop properties, climate, and management systems (Table 1). Values of these parameters can be easily obtained from literature and Canadian databases (e.g., NSDB and ECCC), which was the intent of developing the model. Potential sources and references for obtaining these parameters are also listed in Table 1 should they not be available locally. Appendix D presents the soil hydraulic properties reported in the literature for various soil types. Apart from precipitation, the minimum required climate input to run the model is temperature in order to calculate ET_R using the Hargreaves-Samani equation. Initial soil moisture content of each soil layer (soil moisture content at the start of the simulation period) is also required as input to the model. If measured values of these parameters are not available, moisture content at field capacity would be a reasonable assumption for irrigated fields, while for rainfed fields (depending on precipitation events and amounts prior to seeding), field capacity can be assumed for wet weather and 50 % of total available water for dry weather conditions.

Outputs from the model include actual evaporation/evapotranspiration, surface runoff, deep percolation, and changes in water storage (Table 1).

2.3. Sequence of model calculation

The model can run in multiple years on a daily time step. It is suggested to start simulation a few days before seeding. As the model does not simulate soil freeze/thaw dynamics, it is not recommended to start simulation during non-growing or dormant periods (i.e., when soil is frozen).

The different water budget components are added to or removed from the soil profile (control volume) sequentially (Fig. 3). Calculation starts off with sublimation (if applicable) and the remaining amount of water in the snow pack is then used to calculate snow accumulation or melt (depending on air temperature). This is followed by the calculation of runoff (from rain and snowmelt) and infiltration of water to the first soil layer. It is assumed that there is no runoff from irrigation, i.e., 100 % of the irrigation water infiltrates into the soil. Percolation of water to each succeeding soil layer is then simulated followed by the removal of water through evaporation/evapotranspiration. Moisture content of the soil profile is updated after every addition or removal of a water budget component.

Table 1
Model input requirements and outputs.

Model inputs	
a.	Site • Parameters: latitude, elevation • Potential sources: local data
b.	Soil • Parameters: soil type, field capacity, wilting point, saturation, saturated hydraulic conductivity • Potential sources: local data, NSDB, pedotransfer functions (Saxton and Rawls, 2006)
c.	Management systems • Parameters: cover type, treatment/management systems • Potential sources: local data
d.	Curve number • Potential source: United States Department of Agriculture (USDA) (2021)
e.	Climate • Parameters: precipitation, temperature, wind speed, relative humidity, solar radiation • Potential sources: local data, ECCC
f.	Crop • Parameters: planting/harvest dates, rooting depth, root distribution, crop coefficient • Potential sources: local data, FAO56 (Allen et al., 1998), AIMM (Alberta Agriculture and Forestry, 2020)
g.	Initial soil moisture content • Potential sources: local data, assumptions (e.g., field capacity)
Model outputs	Evaporation/evapotranspiration, surface runoff, deep percolation, soil moisture content

Acronyms: AIMM – Alberta Irrigation Management Model; ECCC – Environment and Climate Change Canada; FAO – Food and Agriculture Organization; NSDB – National Soil DataBase.

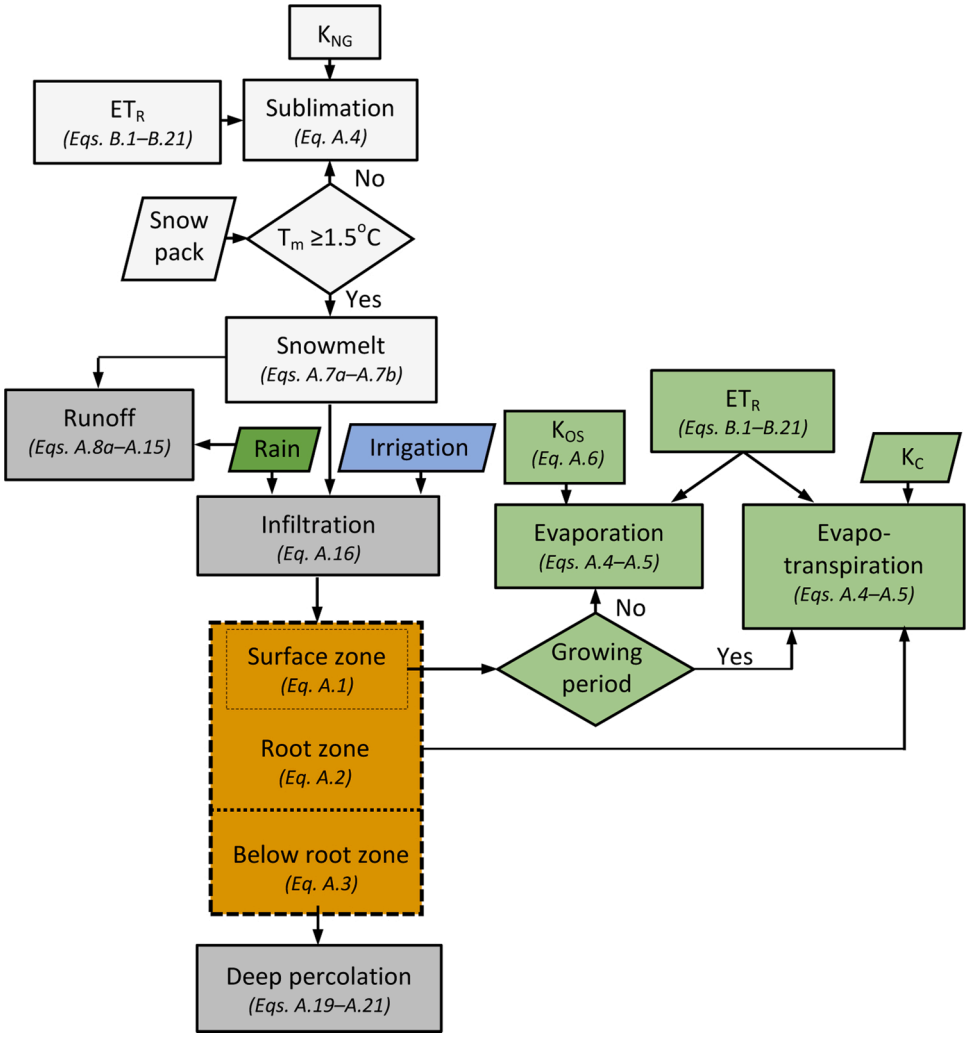

Fig. 3. Flow diagram for the hydrologic calculations implemented in the model.

2.4. Field measurements for model testing

2.4.1. Kenton and Carberry sites

The two sites in Manitoba (Kenton and Carberry sites; Fig. 4) were characterized by sub-humid climatic conditions. The soils at the

Fig. 4. Locations of field sites in provinces of Manitoba and Prince Edward Island (PE), Canada.

two sites had clay loam surface textures and were classified as Black Chernozem according to the Canadian System of Soil Classification (Table 2). The Kenton site was an organic farm situated 50 km northwest of Brandon, Manitoba (50°01′16″ N, 100°34′26″ W). It was sown with millet and hemp in June of 2013 and 2014, respectively, and with fall rye in September 2014. The Carberry site was a conventional crop production field at the Canada-Manitoba Crop Diversification Centre-Carberry located approximately 45 km east of Brandon, Manitoba (49°54′22″ N, 99°20′49″ W). This site was planted with soybean, spring wheat, and canola in the 2013, 2014, and 2015 growing seasons, respectively. Daily meteorological data, which included maximum and minimum temperature, maximum and minimum relative humidity, incoming solar radiation, wind speed, precipitation, and sensible heat flux were monitored at both sites as described in Martel et al. (2018). Sensible heat flux was measured directly at each site using sonic anemometer-thermometers (81000, R.M. Young Company, Traverse City, MI at Kenton site; CSAT3, Campbell Scientific, Inc., Logan, UT at Carberry site) and the eddy covariance technique. Daily ET_C rates were estimated using the residual energy balance (REB) technique (Martel et al., 2018) and soil moisture contents were measured at 20, 50, and 100 cm depths using soil moisture probes (Table 3). As the probes (Model 5 T M, Decagon Devices Inc., Pullman, WA) were calibrated for liquid water and not for ice, the soil moisture measurements when the soil was frozen were excluded in the data analysis for soil moisture content. Deep percolation was measured using a Gee passive capillary lysimeter (G2 Drain Gauge, Decagon Devices Inc.) installed at each field site in fall 2012 near the REB system and collocated with the soil moisture profile. The divergence control tubes (0.2 m diameter, 0.66 m length) of the lysimeter assemblies were installed such that the tops were located 0.5 m beneath the soil surface and bottoms at a depth of 1.2 m. The volume of water exiting through the bottom of each lysimeter divergence control tube was monitored using a level sensor (drainage resolution ±0.1 mm) and logged electronically (Em50 data logger, Decagon Devices Inc.). Runoff volume was measured at edge-of-field of each site using compound sharp-crested v-notch weirs as described in Wilson et al. (2019). Both fields were non-irrigated during the study period. Further, there were no surface drains or ditches at these two sites.

2.4.2. Harrington site

The climate in Harrington, Prince Edward Island was classified as humid continental. The study was conducted at the experimental farm of the Agriculture and Agri-Food Canada, located 10 km north of Charlottetown (46°20′37″ N, 63°10′11″ W) (Fig. 4; Table 2). The soil at the site had a sandy loam surface texture, and was classified as Ferro-Humic Podzol according to the Canadian System of Soil Classification (Nyiraneza et al., 2015). The field was under a 3-year potato rotation [potato – barley (underseeded with clover) – clover]; however, only the potato data in 2011 and 2014 were used in the analysis due to availability of the crop coefficient. Daily soil moisture was measured at the site at 5, 20, 30, 50, and 80 cm depths using soil moisture probes (capacitance/frequency domain sensor) (Table 3) (Danielescu et al., 2016). Temperature and precipitation data were taken from the Environment Canada data from its Charlottetown station. Runoff, deep percolation, and ET were not measured at this site. The field was also non-irrigated, and similar to the other two study sites, there were no surface drains/ditches at this site.

2.5. Sensitivity and uncertainty analyses

A global first-order sensitivity analysis was conducted to assess the influences of field capacity, wilting point, saturation, saturated hydraulic conductivity, maximum root depth, curve number (CN), and crop coefficient on model outputs using a variance-based approach (Saltelli et al., 2008) described in Eq. (1).

$$S_i = \frac{V[E(Y|X_i)]}{V(Y)} \tag{1}$$

where Y and X represent output and input variables, respectively. S_i denotes first-order sensitivity index for parameter X_i, $E(Y|X_i)$ is the expected value of the output Y keeping X_i fixed, averaged over all possible values of non-X_i factors, and $V(Y)$ is the total output variance of output Y. The conditional variance $V[E(Y|Xi)]$ was calculated across all values of X_i. S_i in Eq. (1) represents the fractional contribution of the conditional variance due to parameter X_i to the unconditional variance of the model. Higher S_i indicates greater influence on the output. A sample size of 100, equivalent to 10,000 model runs, was randomly generated for each abovementioned model parameter, which was assumed to be uniformly distributed within the upper and lower bounds (±20 % of the default values for all parameters, except for CN, which was ±10 %) listed in Table 4. The sensitivity of the model was evaluated using potato as the crop

Table 2
Location, climate normal, and crops grown at the study sites.

Site	Location			Crop	Treatment	Soil type (top layer)	Climate normal[a]	Reference
	Province	Latitude	Longitude				30-yr (1981−2010) T, P, RH	
Carberry	MB	49°54′ N	99°20′W	S-SW-C	CM	CL	2.2 °C, 474 mm, 72 %	Martel et al. (2018)
Kenton	MB	50°01′ N	100°34′W	M-H-FR	OM	CL		Martel et al. (2018)
Harrington	PEI	46°20′N	63°10′W	P	CM	SL	5.7 °C, 1158 mm, 77 %	Danielescu et al. (2016)

Acronyms: S – soybean; SW – spring wheat; C – canola; M – millet; H – hemp; FR – fall rye; CM – conventional management; OM – organic management; P – potato; CL – clay loam; SL – sandy loam.

[a] http://climate.weather.gc.ca.

Table 3
Water budget components measured at the research sites, with the methods and periods of measurement.

Site	Water budget component measured				Measurement methods	Period (DD/MM/YEAR)	Reference
	ET	RO	DP	SM		Start – End	
Carberry	✓	✓	✓	✓	REB (ET), weirs (RO), lysimeters (DP), capacitance/frequency domain sensor (SM)	01/05/2013 – 31/10/2015	Martel et al. (2018)
Kenton	✓	✓	✓	✓	REB (ET), weirs (RO), lysimeters (DP), capacitance/frequency domain sensor (SM)	01/05/2013 – 31/10/2015	Martel et al. (2018)
Harrington				✓	capacitance/frequency domain sensor (SM)	28/05/2011 – 31/10/2011 01/05/2014 – 31/10/2014	Danielescu et al. (2016)

Acronyms: ET – evapotranspiration; RO – runoff; DP – deep percolation; SM – soil moisture; REB – residual energy balance.

under two different conditions: sub-humid (Kenton site; using the 2015 weather data) and humid (Harrington site; using the 2011 weather data).

An uncertainty analysis was performed to quantitatively evaluate the model estimates using the average deviation amplitude (ADA) index [Eq. (2)] implemented in other studies (Xiong et al., 2009; Walega and Ksiazek, 2016).

$$ADA = \frac{1}{n}\sum_{t=1}^{n}\left|\frac{1}{2}(UL_t + LL_t) - O_t\right| \tag{2}$$

where n is the number of days considered in the analysis, UL_t is the 95th percentile of the simulated data at day t, LL_t is the 5th percentile of the simulated data at day t, and O_t is the observed data at day t. Lower ADA values indicate lower uncertainty.

2.6. Statistical analysis

Statistical approaches were used to quantitatively assess the performance of the model by comparing measured and simulated values. The statistical measures implemented include Nash–Sutcliffe model efficiency coefficient (NSE), index of agreement (d), root mean square error (RMSE), average relative error (ARE), and coefficient of determination (R^2) (Eqs. 3–7).

$$NSE = 1.0 - \frac{\sum_{i=1}^{n}(O_i - P_i)^2}{\sum_{i=1}^{n}\left(O_i - \overline{O}\right)^2} \tag{3}$$

$$d = 1 - \frac{\sum_{i=1}^{n}(P_i - O_i)^2}{\sum_{i=1}^{n}\left(\left|P_i - \overline{O}\right| + \left|O_i - \overline{O}\right|\right)^2} \tag{4}$$

$$RMSE = \left[\frac{\sum_{i=1}^{n}(O_i - P_i)^2}{n}\right]^{0.5} \tag{5}$$

$$ARE = \frac{\sum_{i=1}^{n}(P_i - O_i)}{n \cdot \overline{O}} \tag{6}$$

$$R^2 = \left(\frac{\sum_{i=1}^{n}\left(O_i - \overline{O}\right)\cdot(P_i - \overline{P})}{\sqrt{\sum_{i=1}^{n}(P_i - \overline{P})^2 \cdot \sum_{i=1}^{n}(O_i - \overline{O})^2}}\right)^2 \tag{7}$$

where O and P refer to the observed and modeled values, respectively, n is the number of observations, and the overbar indicates mean value.

The value of NSE ranges from negative infinity to 1.0, where a NSE = 1.0 indicates a perfect fit, while a NSE $\leq$ 0 indicates that the observed mean is better than the model prediction (Ritter and Muñoz-Carpena, 2013). The indicators RMSE and ARE summarize the mean difference between measured and modeled values, and the smaller the difference, the better is the agreement between the two. Values closer to 1.0 for d and R^2 indicate better agreement between measured and modeled values.

Table 4
Upper and lower bound values of the parameters used in the sensitivity analysis.

Soil layer depth	FC (mm/m)		WP (mm/m)		Saturation (mm/m)		K_{sat} (mm/m)		Z_{max} (m)		K_C (-)										CN (-)	
											$a/10^{-2}$		$b/10^{-3}$		$c/10^{-6}$		$d/10^{-9}$		$e/10^{-13}$			
	U	L	U	L	U	L	U	L	U	L	U	L	U	L	U	L	U	L	U	L	U	L
Kenton site																						
Layer 1	312	208	157	105	626	418	361	241														
Layer 2	350	234	205	137	541	361	134	89	0.6	0.4	6.7	4.5	2.1	1.4	−2.3	−1.5	1.8	1.2	−6.5	−4.3	94	77
Layer 3	350	234	205	137	541	361	134	89														
Layer 4	305	203	184	122	492	328	141	94														
Harrington site																						
Layer 1	276	184	150	100	506	338	5868	3912														
Layer 2	312	208	218	146	545	363	2737	1825	Same as in Kenton site		Same as in Kenton site										89	73
Layer 3	336	224	222	148	566	378	2042	1362														
Layer 4	336	224	222	148	566	378	2042	1362														

FC – field capacity; WP – wilting point; K_{sat} – saturated hydraulic conductivity; Z_{max} – maximum root depth; K_C – crop coefficient; CN – curve number; U – upper bound; L – lower bound; a, b, c, d, and e are crop coefficients.

3. Results

3.1. Sensitivity of model outputs to key parameters and uncertainty of model results

Results of the sensitivity analysis show that for both Kenton and Harrington sites the most influential factor for ET and runoff were K_C and CN, respectively (Table 5). The CN also had a slight influence on deep percolation in both sites. The most influential factor for deep percolation in Kenton site was field capacity, while that in Harrington site was K_C. On the contrary, the most influential factor for soil moisture content in Kenton site was K_C, while that in Harrington site was field capacity. Wilting point, saturation, saturated hydraulic conductivity, and maximum root depth did not show substantial influence on any of the model outputs in the tested range.

The uncertainty of the model results, indicated by the ADA values (Table 6), are comparable with those obtained in other hydrological modeling studies (Xiong et al., 2009; Walega and Ksiazek, 2016).

3.2. Measured and estimated water budgets

On average, the estimated evapotranspiration to precipitation ratio (ET_R:P) in Carberry and Kenton sites (sub-humid climate) was 1.5, while that in Harrington (humid continental) was 0.8 (Table 7). The relatively high precipitation in Kenton site in 2014 was mostly due to a series of heavy rainfall events, which deposited 115 mm of rain over four days in early summer (June 27 – June 30). Although 2013 was a drier year on an annual basis compared to 2014, both Kenton and Carberry sites experienced 96 mm of rain from June 22–June 26 in 2013. It should be noted that for 2013 and 2015, only a portion of the year was considered in the study (see Table 3).

Measured annual cumulative actual evapotranspiration, runoff, and deep percolation in Carberry and Kenton sites ranged from 409 to 534 mm, 0 to 61 mm, and 0 to 172 mm, respectively, while simulated values ranged from 383 to 475 mm, 0 to 28 mm, and 0 to 150 mm, respectively (Fig. 5). Measured ET, runoff, and deep percolation in Carberry site accounted for 95 %, 4 %, and 1 %, respectively, of the total water flow balance while simulated values accounted for 96 %, 4 %, and 0 %, respectively. In Kenton site, measured ET, runoff, and deep percolation accounted for 84 %, 3 %, and 13 %, respectively, of the total water flow balance compared with the simulated values, which accounted for 81 %, 4 %, and 15 %, respectively.

As the fields were non-irrigated, the difference between total inflow (i.e., precipitation in Table 7) and total outflow (i.e., evapotranspiration + runoff + deep percolation; Fig. 5) could be assumed to represent the net change of soil moisture. Simulated net change of soil moisture in Carberry and Kenton sites were 18 and -146 mm, respectively, indicating that the estimated water budgets balanced well for both sites.

3.3. Model performance

The model estimated daily ET relatively well, with *d* values ranging from 0.7–0.9 for Kenton site and 0.6–0.8 for Carberry site for the various periods (Table 8). It underestimated ET during the growing and non-growing/dormant periods by approximately 19 % and 21 %, respectively, in Kenton site and 20 % and 7%, respectively, in Carberry site; however, it overestimated ET during pre-planting/post-harvest by 12 % in Kenton site and 42 % in Carberry site. As the pre-planting and post-harvest were relatively shorter periods compared to the other, the model tended to generally underestimate ET in both sites (Figs. 6 and 7).

Overall, the model simulated daily deep percolation during the various periods relatively well as explained by the lower RMSE and ARE values shown in Table 8. In particular, it showed better performance for Carberry site than Kenton site. It should be noted that the 100 % ARE obtained for Carberry site during the growing season resulted from a 14 mm deep percolation measured over four days against zero millimeters estimated by the model (Fig. 8c and d). Most of the discrepancy in deep percolation in Kenton site in 2013 occurred in the month of June when a 96 mm of rain deposited over six days (June 24 to June 30) resulted in a deep percolation of 77 mm, yet, the model predicted only a total of 27 mm deep percolation (with only 1 mm runoff) for the same period (Fig. 9c and d). No runoff was observed during this period (Fig. 9a). Most of the rain resulted in an increase in the simulated soil moisture. In the following year, at the same site, the model estimated a total of 82 mm deep percolation and 9 mm runoff from June 27 to June 30 after a 115 mm rainfall; however, only 4 mm deep percolation and 2 mm runoff were observed during this period. Increases in soil moisture content

Table 5
First-order sensitivity indices for the various parameters.

Input parameter	ET		RO		DP		SW	
	Kenton	Harrington	Kenton	Harrington	Kenton	Harrington	Kenton	Harrington
FC	0.033	0.012	0.008	0.002	0.517	0.068	0.015	0.986
WP	0.059	0.007	0.023	0.039	0.115	0.024	0.059	0.000
Sat	0.001	0.000	0.024	0.062	0.009	0.016	0.001	0.000
K_{sat}	0.000	0.000	0.000	0.000	0.000	0.000	0.000	0.000
CN	0.069	0.000	0.910	0.844	0.163	0.222	0.044	0.000
Z_{max}	0.010	0.003	0.001	0.001	0.001	0.005	0.018	0.000
K_C	0.828	0.978	0.034	0.052	0.195	0.665	0.862	0.014

ET – evapotranspiration; RO – runoff; DP – deep percolation; SW – soil moisture content; FC – field capacity; WP – wilting point; Sat – saturation; K_{sat} – saturated hydraulic conductivity; CN – curve number; Z_{max} – maximum root depth; K_C – crop coefficient.

Table 6
Average deviation amplitude (ADA) values from uncertainty analysis.

	ET			RO			DP			SM
	PP/PH	NG/D	G	PP/PH	NG/D	G	PP/PH	NG/D	G	
Carberry	0.84	0.11	0.94	0.25	0.05	0.21	0.00	0.00	0.04	0.02
Kenton	0.44	0.09	0.87	0.39	0.14	0.07	0.60	0.00	0.48	0.01
Harrington	–	–	–	–	–	–	–	–	–	0.03

PP/PH – pre-planting/post-harvest; NG/D – non-growing/dormant; G – growing.
The symbol "- "means no data available.

Table 7
Precipitation (P) and estimated evapotranspiration (ET_R) at the study sites for the period presented in Table 3.

Site	Carberry			Kenton			Harrington	
Period	2013	2014	2015	2013	2014	2015	2011	2014
Precipitation (mm)	481	509	462	423	609	403	635[a]	537[a]
ET_R[b] (mm)	**603**	**731**	**790**	**663**	**735**	**787**	–	–
	598	698	763	641	678	762	436	550
ET_R:P	1.3	1.4	1.7	1.6	1.2	2.0	0.7	1.0

[a] Precipitation taken from Environment Canada data measured at Charlottetown, PEI station.

[b] ET_R was estimated as reference evapotranspiration when the Penman-Monteith equation was used (bold font) and as potential evapotranspiration when the Hargreaves-Samani equation was used.

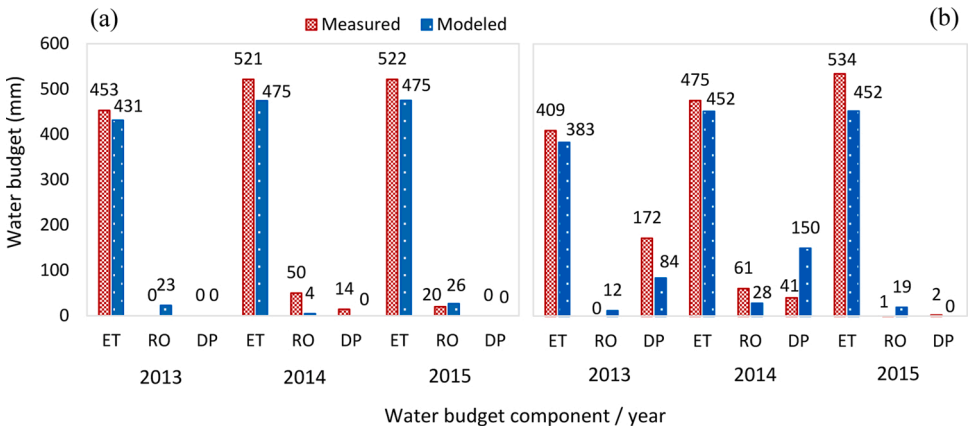

Fig. 5. Comparison between measured and estimated annual evapotranspiration, runoff, and deep percolation in (a) Carberry and (b) Kenton sites from May 2013 – October 2015.

were observed at the site.

Although the model tended to overestimate runoff during the growing season, the *d* statistic, which ranged from 0.5–0.8 (Table 8) suggests a relatively good performance. The 272 % ARE obtained in Kenton site resulted from the cumulative 10 mm runoff estimated by the model against the 3 mm observed in the site over the three growing periods, while the 178 % in Carberry site resulted from the cumulative 36 mm estimated by the model against 13 mm measured runoff. The model also showed a relatively good performance for the non-growing/dormant period as explained by the relatively lower RMSE values (0.4–0.6 mm/d). However, relatively large inconsistencies in runoff were observed during pre-planting/post-harvest, particularly at the beginning of spring when the snow started to melt (Figs. 8a and b and 9 a and b).

There was a relatively good agreement between simulated and observed soil moisture content with ARE ranging from -0.4 %–21.0 % and *d* ranging from 0.4–0.8 (Table 9). It should be noted that the data when the soil was frozen were not included in the analysis for Kenton and Carberry sites, as mentioned in the Method section. Although the model tended to overestimate the moisture content in upper layers and underestimate in lower layers, it was able to capture the peaks, particularly in the upper layers (Fig. 10).

Table 8
Statistical performance of the model for evapotranspiration (ET), runoff (RO), and deep percolation (DP) in Carberry and Kenton sites for the various periods using the data collected from May 2013 to October 2015.

Statistical index	Water budget component																	
	Carberry									Kenton								
	ET			RO			DP			ET			RO			DP		
	PP/PH	NG/D	G	PP/PH	NG/D	G	PP/PH	NG/D	G	PP/PH	NG/D	G	PP/PH	NG/D	G	PP/PH	NG/D	G
R^2 (-)	0.3	0.5	0.4	0.0	0.0	0.6	–	–	–	0.6	0.6	0.4	0.0	–	0.8	0.0	–	0.0
RMSE (mm/d)	1.2	0.3	1.4	2.0	0.4	0.6	0.0	0.0	0.4	0.8	0.4	1.3	2.2	0.6	0.4	3.5	0.0	3.2
d (-)	0.6	0.7	0.8	0.1	0.1	0.8	–	–	0.0	0.9	0.7	0.8	0.0	0.0	0.5	0.2	–	0.3
NSE (-)	−1.4	0.4	0.3	0.0	−1.1	0.3	–	–	0.0	0.5	0.4	0.1	−0.1	–	−16.0	−1.5	–	−1.4
ARE (%)	42.0	−7.0	−19.8	−81.2	9.4	178.3	–	–	−100.0	12.3	−21.2	−19.2	−52.2	–	271.6	−7.5	–	26.9

PP/PH – pre-planting/post-harvest; NG/D – non-growing/dormant; G – growing.
The symbol "- "indicates that either the measured or both measured and simulated values are zero.

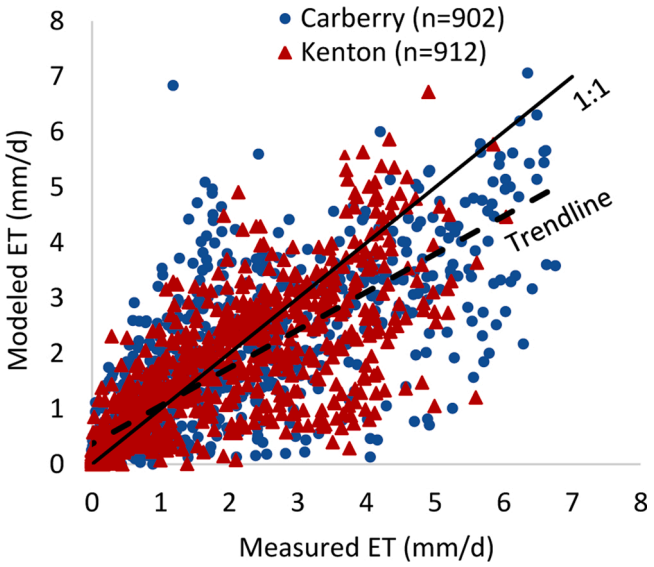

Fig. 6. Simulated versus measured evapotranspiration at Carberry and Kenton sites throughout the simulation period at daily resolution.

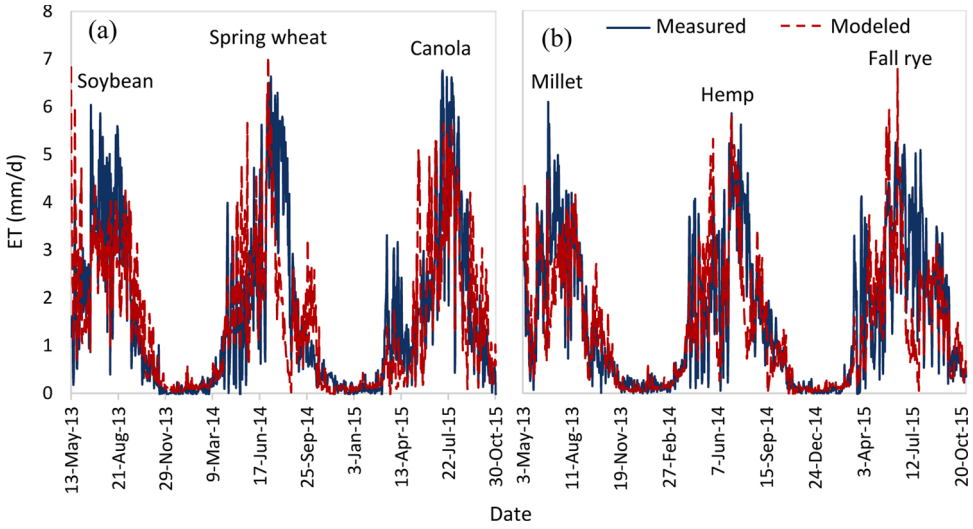

Fig. 7. Daily time series of simulated and measured evapotranspiration in (a) Carberry and (b) Kenton sites throughout the simulation period.

4. Discussion

4.1. Sensitivity of model outputs to key parameters

The high influence of K_C on ET was not surprising considering that ET was estimated from these coefficients. This suggests that more accurate and representative crop/surface coefficients are necessary for better ET estimates. The high sensitivity of runoff to CN found in this study agrees with what other studies have also observed. Soomro et al. (2019) obtained a 78 % reduction in peak discharges when the CN value was reduced from 90 to 40. In addition, Boughton (1989) found that increasing CN by 15 %–20 % doubled the estimated runoff, while reducing CN by the same range reduced runoff by half. Hawkins (1975) found that runoff was more sensitive to CN than to rainfall even with rainfall of up to 229 mm. This indicates that accurate CN values are crucial for estimating runoff that employs the NRCS-CN method. The sensitivity of runoff to CN even at very small variations could be the downside of this method as the differences between some of the CN_{II} values provided in the NRCS hydrology national engineering handbook for various soil groups and land covers are relatively large. Thus, choosing a slightly different CN value could result in a large error in runoff. The slight influence of CN on deep percolation could be due to its influence on runoff as changes in runoff may also impact deep percolation. The differing impacts of field capacity and K_C on deep percolation and soil water content in Harrington and Kenton sites could

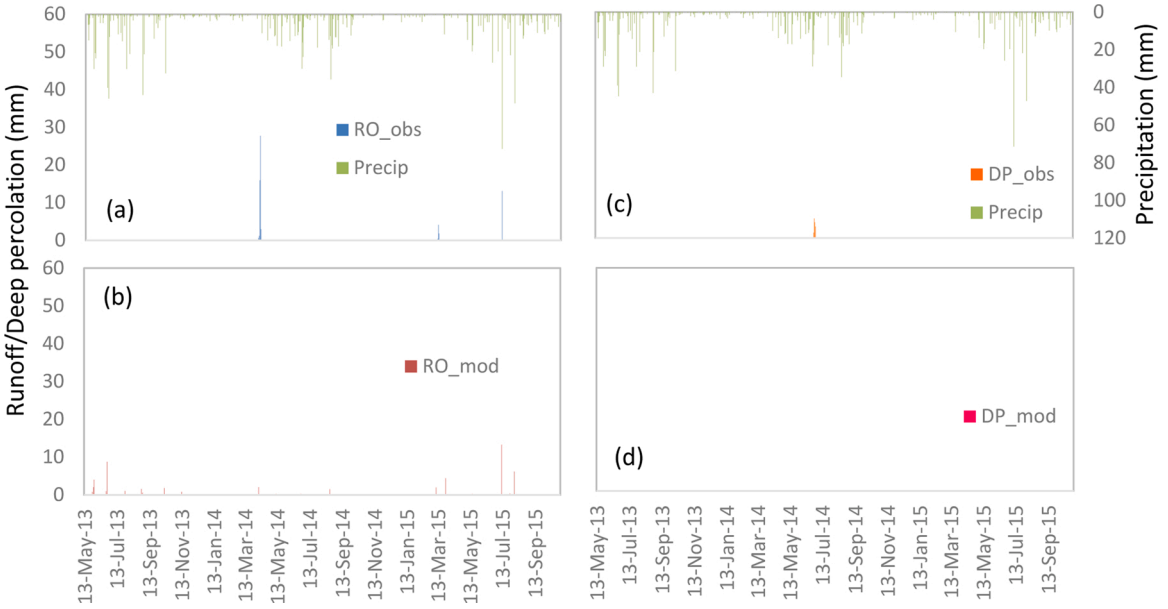

Fig. 8. (a) Observed and (b) simulated runoff; (c) observed and (d) simulated deep percolation at the Carberry site.

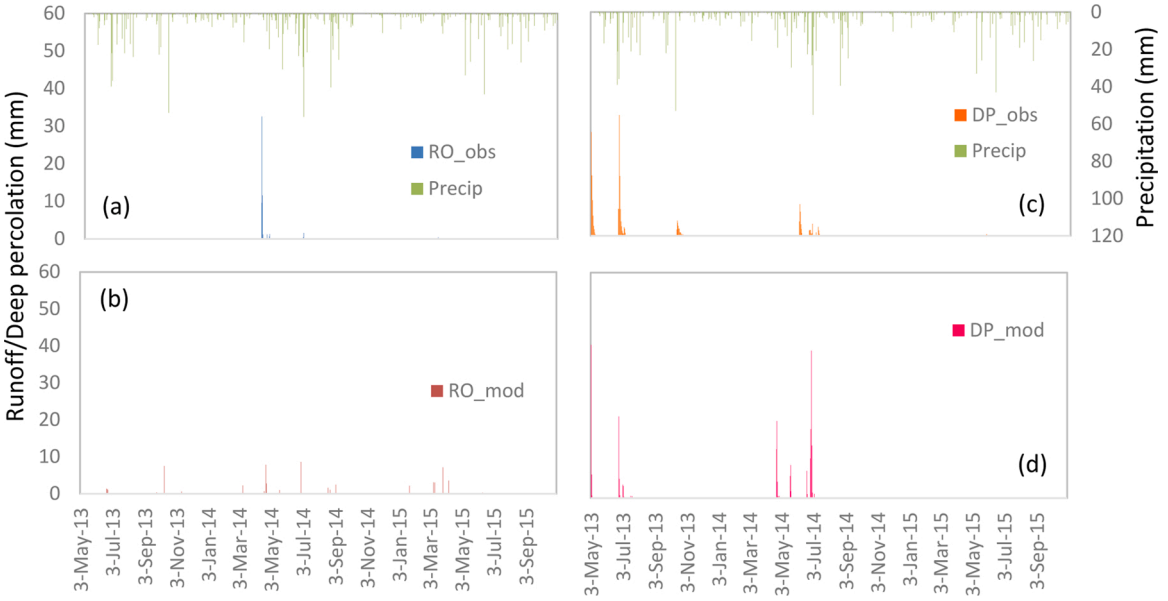

Fig. 9. (a) Observed and (b) simulated runoff; (c) observed and (d) simulated deep percolation at the Kenton site.

be due to the difference in the precipitation to evapotranspiration ratio in these sites. Varying the field capacity did not have a substantial impact on deep percolation in Harrington site as the high precipitation in the site always resulted in deep percolation whether field capacity was high or low; however, it affected moisture content as field capacity is the amount of water held in soil after excess water has drained away. On the contrary, due to the semi-arid condition in Kenton site, varying the field capacity of the soil resulted in substantial impact on deep percolation. Crop coefficients did influence deep percolation in Harrington site probably due to their slight impact on soil moisture content. Root depth did not have influence on deep percolation probably due to relatively shorter root depths (0.4–0.6 m) employed in the analysis. Saturation did not show any influence on the model outputs as the simulated soil moisture content in both sites did not reach the saturation of the soil. In addition, it was found that saturated hydraulic conductivity had to be very low (such as those of a clay soil) to have substantial influence on the model outputs.

Table 9
Statistical performance of the model for soil moisture.

Statistical index	Carberry site				Kenton site				Harrington site			
	0−20 cm	20−50 cm	50−75 cm	75−100 cm	0−20 cm	20−50 cm	50−75 cm	75−100 cm	0−10 cm	10−20 cm	20−30 cm	30−50 cm
R^2 (-)	0.05	0.09	0.09	0.05	0.40	0.55	0.54	0.42	0.34	0.25	0.05	0.03
RMSE (vol. fraction)	0.06	0.04	0.06	0.06	0.03	0.03	0.04	0.03	0.04	0.03	0.04	0.05
d (-)	0.46	0.53	0.47	0.48	0.79	0.82	0.77	0.77	0.66	0.65	0.53	0.41
NSE (-)	−2.13	−1.88	−4.77	−1.67	0.11	−0.03	−0.56	0.06	−0.32	−0.04	−0.58	−2.28
ARE (%)	−6.40	−0.39	−12.90	−21.02	0.35	−4.02	−7.40	−6.05	8.31	0.40	2.03	3.65

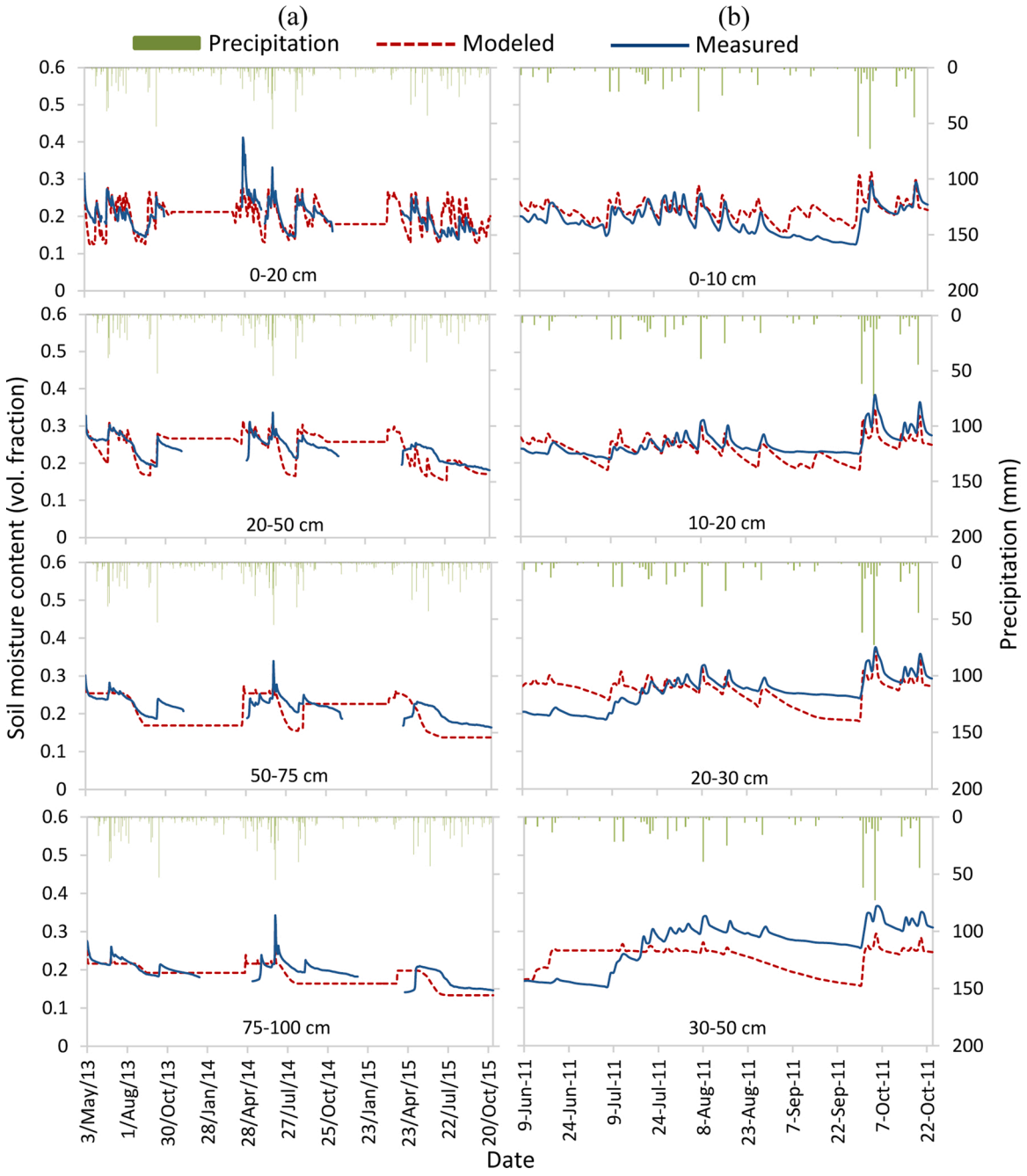

Fig. 10. Daily time series of simulated and measured soil moisture content at (a) Kenton site (May 2013 – October 2015) and (b) Harrington site (June 2011 – October 2011). Soil moisture measurements at Kenton site when soil temperatures were equal or below 0 °C were excluded as the probes were not calibrated for frozen soils.

4.2. Model performance

As ET was mainly influenced by K_C, as indicated by the results of the sensitivity analysis, the varied performance of the model in estimating ET for the different periods (underestimate in growing and non-growing/dormant and overestimate in pre-planting/post-harvest periods) could be due to the different crop and surface coefficients used in the model for the various periods, which were not calibrated as part of the modeling approach and objective of the study. Most of the underestimates during growing period occurred toward the end of the period (Fig. 7). Using the SWAT model, Marek et al. (2016) also observed underestimates in ET toward the end of the growing period of sorghum, which coincided with the underestimates in leaf area index. The underestimates in soil moisture

content available for root uptake at deeper soil layers toward the end of the growing period (Fig. 10) could also be the reason for the underestimates in ET. In addition, the inconsistency in ET could also be due to the conversion of the alfalfa-based K_C and application of these coefficients in the Penman-Monteith equation, which was developed for grass-based K_C. The discrepancy in ET during the non-growing/dormant and pre-planting/post-harvest periods could be due to the wide fluctuation in temperature at the beginning and end of these periods. For instance, in April 2014, the model was already simulating pre-planting (which has higher ET than for non-growing period) in Carberry and Kenton sites as the criterion of five consecutive daily temperatures of 0 °C or below was no longer satisfied; yet, there were a couple of days during this month where the measured T_{min} were still as low as -15 °C and −11 °C (with a few snow falls) for the two sites, respectively. This means that due to the abovementioned criterion, the model could be using the pre-planting/post-harvest surface coefficient even when the temperature was below 0 °C or using the non-growing/dormant surface coefficient even the temperature was above 0 °C. Hence, most overestimates were observed during the months of April, May, and October (Fig. 7). Regardless of the identified errors, the performance of the model in simulating ET even without calibration was comparable to that of a calibrated/validated SWAT model, which obtained RMSE values ranging from 1.18 to 1.48 mm/day for growing cotton, grain sorghum, soybean, and from 0.63–0.82 mm/day for non-growing season (Marek et al., 2016). Higher RMSE values were obtained for growing period, which was likely due to greater crop water demand during this period. The model performance on estimating ET is comparable with those of other models [DNDC: $d = 0.83$ and VSMB: $d = 0.72$ (Guest et al., 2018); improved version of DNDC: $R^2 = 0.73–0.85$ and RMSE = 0.77–1.04 mm/d (Dutta et al., 2016); RZWQM2: RMSE = 1.0–1.5 mm/d (Anapalli et al., 2016); SWAT: $R^2 = 0.81$ (Melaku and Wang, 2019); Hydrus 2D/3D: $R^2 = 0.51–0.78$) (Mante and Ranjan, 2017)].

The model simulated deep percolation relatively better in Carberry site than in Kenton site. One of the main differences between these two sites were the weeds and volunteers that deliberately grew in Kenton site; however, as ET and soil moisture content were simulated relatively better in Kenton site than in Carberry site as indicated by higher R^2, d, and ARE statistics, the presence of weeds and volunteers might not be the cause for the larger error in deep percolation in Kenton site. The discrepancy could be due to the inaccuracy of the water holding capacity, particularly field capacity, of which deep percolation was highly sensitive to (sensitivity index of 0.52; Table 5). Its impact on deep percolation seemed to be more pronounced during periods of heavy rain. In addition, the inconsistency in deep percolation could also be due to the relatively poor performance of the model for runoff, particularly during spring. In Kenton site for instance, a total of 55 mm runoff was observed in early April 2014 from snowmelt; however, no runoff from snowmelt was predicted during this period. The model captured the snowmelt towards the end of that month, which resulted in a total of 39 mm deep percolation. Evaluating the model performance on a long-term basis (e.g., monthly, yearly), as what other studies have done (Tafteh and Sepaskhah, 2012; Mapes and Pricope, 2020), could have resulted in better agreement as it could eliminate the error caused by the difference in the timing of occurrence.

As mentioned above, a relatively large discrepancy was observed between simulated and measured runoff, particularly those from snowmelt, which resulted in relatively poor performance statistics for pre-planting/post harvest period (Table 8; Figs. 8a and b; 9 a and b). For instance, a total of 49 mm runoff from snowmelt was observed in the beginning of April 2014 in Carberry site; however, the model estimated only 2 mm as mean air temperatures were still below 1.5 °C. It should be noted that in the model, snowmelt occurs only when mean air temperature is $\geq$ 1.5 °C. Similar phenomenon was also observed in Kenton site in the same period, as described earlier. Though temperature-based snowmelt equation is simple to implement, the melting factor and base temperature used in this equation are dependent on several factors, including snow density, liquid water content, thermal conductivity, snow albedo, and wind speed (Kondo and Yamazaki, 1990; USDA, 2004). Variations of these factors can change the energy dynamics and snowpack conditions over time and space. Massmann (2019) found that temperature-based snowmelt models give good results in gauged basins, but not in ungauged ones due to lack of data for calibration of the snowmelt parameters. The results of this study suggest necessary improvements for the snowmelt algorithms. The error in runoff estimates during the growing period could be due to the NRCS-CN method employed. Numerous studies have shown that the CN values provided in the NRCS hydrology national engineering handbook can be substantially different from those calculated using observed rainfall-runoff events (Tedela et al., 2012; Kowalik and Walega, 2015; Lal et al., 2017; Walega and Salata, 2019). Results from the sensitivity analysis conducted in this study, as well as from other related studies (Hawkins, 1975; Boughton, 1989), show that even a small difference in CN value can result in substantial difference in runoff. Further, several studies have indicated that the 0.2 value for initial abstraction adopted in the NRCS-CN method is not always suitable for different site-specific cases (D'Asaro and Grillone, 2012; Ling and Yusop, 2014). Moreover, Garen and Moore (2005) underlined that the NRCS-CN procedure was originally developed at a watershed scale; thus, it is not suitable for point, plot, or field scale applications. However, despite the limitations of the CN method, it has been employed in many hydrological models (e.g., DNDC, SWAT, PRZM, and VSMB) due to its simplicity and dependence on a few parameters only (Ponce and Hawkins, 1996); hence, it is the one adopted in the model. Regardless of this limitation, the d statistic of the model for growing period is comparable to the 0.55 and 0.64 of the RZWQM and DNDC models, respectively (Smith et al., 2020) and the 0.49 of the VSMB model (Guest et al., 2018).

As the model does not simulate soil freeze/thaw dynamics, and allows infiltration and water movement in soil based only on air and soil surface temperatures, the simulated increases in moisture content after winter generally occurred a few days earlier than were observed. The model tended to overestimate moisture content in upper layers, but underestimate moisture content in lower layers (Fig. 10), which is a common issue with bucket models as they do not simulate unsaturated downward flow of water. Smith et al. (2019) also observed overestimates in soil moisture content near soil surface and underestimates in the deeper portion of the profile using the DNDC model. Improved root density and penetration functions could improve the results as the authors suggested. In addition, the relatively higher measured moisture contents in the lower layers compared with the modeled values particularly in Harrington site (Fig. 10b) could be due to the upward flow of water, which is not simulated in the model. Presence of a transient perched water table at the bottom of the soil profile has been documented at this site in the past (Zebarth et al., 2015). Factors such as infiltration to frozen soil, preferential flow, and dynamic storage routing, which have been identified to be potentially present in

Manitoba basins (Cordeiro et al., 2017), might have also influenced the simulated soil moisture content. However, the overall performance of the model in simulating moisture content for various soil types is comparable with other models, particularly those that use a cascade flow framework for hydrology. He et al. (2014) obtained RMSE values ranging from 0.02–0.06 (vol. fraction) and *d* values from 0.47–0.90 with a calibrated DSSAT-CERES-Wheat model. DayCent, DNDC, and STICS models obtained ARE ranging from 0.5 %–7.4 % for soil moisture simulations at various sites in eastern Canada (Guest et al., 2017). Wang et al. (2010) obtained R^2 ranging from 0–0.66 using DSSAT and SHAW models.

5. Summary and conclusions

A parsimonious soil water budget model for estimating soil moisture content and water fluxes across agricultural landscapes in Canada was developed by selecting and combining algorithms from various existing models, whose data requirement are readily available in Canadian databases. The model can simulate evapotranspiration, surface runoff, deep percolation, and soil moisture content during various seasons (i.e., growing, non-growing/dormant, and pre-planting/post-harvest) with minimum data requirement, which addresses the limited available data in the country for crop and hydrological modeling.

Sensitivity analysis of the model showed that ET and runoff were highly sensitive to K_C and CN, respectively, indicating the importance of choosing accurate values of these parameters that best represent the field conditions and crop characteristics. It was also found that deep percolation was highly sensitive to field capacity in sub-humid-conditions and to crop coefficient in humid conditions. In contrast, the most influential factor for soil moisture content in sub-humid regions was K_C, while that in humid locations was field capacity.

The model tended to underestimate ET during growing and non-growing/dormant periods, but overestimate ET during pre-planting/post-harvest season; however, despite these inconsistencies, the *d* values ranged from 0.6–0.8, indicating that the model performed relatively well even without site calibration. RMSE values for deep percolation ranged from 0 to 3.5 mm/d, which are comparable with those obtained by other models. The discrepancy in deep percolation could be due to the inaccuracy in field capacity, whose impact became more pronounced during heavy rainfall, and to the inconsistency in simulating runoff from snowmelt. Although the model had a relatively satisfactory *d* statistic for runoff for the growing period, a relatively large inconsistency was observed for runoff from snowmelt, which could be due to the algorithm employed for snowmelt. The discrepancy in runoff could also be attributed to the NRCS-CN method, which seems to be too simplistic in describing actual rainfall-runoff events. Although the model tended to overestimate moisture content in upper layers and underestimate in lower layers, a relatively good agreement was observed between simulated and observed soil moisture content as indicated by relatively lower ARE values, which ranged from -0.4 %–21.0 %. The discrepancy in soil moisture content estimates could be attributed to some soil-water dynamics, which are not considered in the model (e.g., soil freeze/thaw, upward water flow, infiltration to frozen soil, preferential flow, and dynamic storage routing).

Although the model inadequately captured runoff from snowmelt, it simulated soil moisture content, ET, and deep percolation relatively well for its intended simplicity and low-input parameter requirement. The model can run using the GDD-based crop coefficients available for more than 50 crops and widely available soil-water hydraulic and weather parameters. Its overall performance was found comparable with other models, particularly those that implement a cascade flow framework for hydrology. The ADA values indicate that the model simulations have fairly low uncertainties.

Testing the model using the limited amount of data could not sufficiently indicate that the model worked better in one site than the other. Results show that the model, in its current form, is limited by the simplicity of the snowmelt equation and CN method it employs. Better algorithms for snowmelt, improved CN method, and soil freeze/thaw dynamics will be considered for better future estimates. In addition, the implication of using alfalfa-based K_C for the Penman-Monteith equation will be further assessed in the future to carefully consider options and solutions to improve the performance of the model in estimating ET.

CRediT authorship contribution statement

Myra Martel: Conceptualization, Methodology, Writing. **Aaron Glenn**: Investigation, Writing - review & editing. **Henry Wilson**: Investigation, Writing - review & editing. **Serban Danielescu**: Investigation, Writing - review & editing. **Roland Kroebel**: Supervision, Conceptualization, Writing - review & editing. **Ward Smith**: Writing - review & editing. **Brian McConkey**: Writing - review & editing. **Geoffrey Guest**: Methodology. **Henry Janzen**: Supervision.

Declaration of Competing Interest

The authors report no declarations of interest.

Acknowledgements

The authors gratefully acknowledge the support and collaboration of Mr. Ted Harms by providing and allowing them to use the AIMM's crop coefficients. Funding for this research came from AAFC Growing Forward II and Canadian Agricultural Partnership programs.

Appendix A. Supplementary data

Supplementary material related to this article can be found, in the online version, at doi:https://doi.org/10.1016/j.ejrh.2021.100846.

References

Agriculture and Agri-Food Canada (AAFC), 2020. Holos Software Program (Online) [3 Feb. 2021). https://www.agr.gc.ca/eng/scientific-collaboration-and-research-in-agriculture/agricultural-research-results/holos-software-program/?id=1349181297838.

Agriculture and Agri-Food Canada (AAFC), 2021. Canadian Soil Information Service (Online) [10 May 2021). https://sis.agr.gc.ca/cansis/.

Aina, O.O., Dixon, A.G., Akinrinde, E.A., 2007. Effect of soil moisture stress on growth and yield of cassava in Nigeria. Pak. J. Biol. Sci. 10 (18), 3085–3090. https://doi.org/10.3923/pjbs.2007.3085.3090.

Akinremi, O.O., McGinn, S.M., Barr, A.G., 1996. Simulation of soil moisture and other components of the hydrological cycle using a water budget approach. Can. J. Soil Sci. 75, 133–142.

Alberta Agriculture and Forestry, 2020. Alberta Irrigation Management Model (Online) [9 Jan. 2021). https://acis.alberta.ca/imcin/aimm.jsp.

Allen, R.G., Pereira, L.S., Raes, D., Smith, M., 1998. Crop evapotranspiration: guidelines for computing crop water requirements. FAO Irrigation and Drainage Paper No. 56. Food and Agriculture Organization (FAO), Rome, Italy.

Anapalli, S.S., Ahuja, L.R., Gowda, P.H., Ma, L., Marek, G., Evett, S.R., Howell, T.A., 2016. Simulation of crop evapotranspiration and crop coefficients with data in weighing lysimeters. Agric. Water Manag. 177, 274–283. https://doi.org/10.1016/j.agwat.2016.08.009.

Baier, W., Robertson, G.W., 1966. A new versatile soil moisture budget. Can. J. Plant Sci. 46 (3), 299–315. https://doi.org/10.4141/cjps66-049.

Bennett, D.R., Harms, T.E., 2011. Crop yield and water requirement relationships for major irrigated crops in southern Alberta. Can. Water Resour. J. 36 (2), 159–170. https://doi.org/10.4296/cwrj3602853.

Beven, K., Germann, P., 2013. Macropores and water flow in soils revisited. Water Resour. Res. 49, 3071–3092. https://doi.org/10.1002/wrcr.20156.

Boughton, W.C., 1989. A review of the USDA SCS curve number method. Aust. J. Soil Res. 27 (3), 511–523. https://doi.org/10.1071/SR9890511.

Cordeiro, M.R.C., Wilson, H.F., Vanrobaeys, J., Pomeroy, J.W., Fang, X., Red-Assiniboine Project Biophysical Modelling Team, 2017. Simulating cold-region hydrology in an intensively drained agricultural watershed in Manitoba, Canada, using the Cold Regions Hydrological Model. Hydrol. Earth Syst. Sci. Discuss. 21, 3483–3506. https://doi.org/10.5194/hess-21-3483-2017.

D'Asaro, F., Grillone, G., 2012. Empirical investigation of curve number method parameters in the Mediterranean area. J. Hydrol. Eng. 17 (10), 1141–1152. https://doi.org/10.1061/(ASCE)HE.1943-5584.0000570.

Danielescu, S., MacQuarrie, K., Grimmett, M., Sharifi-Mood, N., Power, A., Rodd, V., Nyiraneza, J., Zebarth, B., 2016. A Combined Approach for Understanding Nitrogen Loading to Groundwater From a Field Under Potato Production in Prince Edward Island in Toward Sustainable Groundwater in Agriculture, 28-30 June, San Francisco, California, usa.

Dutta, B., Smith, W.N., Grant, B.B., Pattey, E., Desjardins, R.L., Li, C., 2016. Model development in DNDC for the prediction of evapotranspiration and water use in temperate field cropping systems. Environ. Model. Softw. 80, 9–25. https://doi.org/10.1016/j.envsoft.2016.02.014.

Faramarzi, M., Abbaspour, K.C., Adamowicz, W.L., Lu, W., Fennell, J., Zehnder, A.J.B., Goss, G.G., 2017. Uncertainty based assessment of dynamic freshwater scarcity in semi-arid watersheds of Alberta, Canada. J. Hydrol: Reg. Stud. 9, 48–68. https://doi.org/10.1016/j.ejrh.2016.11.003.

Farthing, M.W., Ogden, F.L., 2017. Numerical solution of Richards' equation: a review of advances and challenges. Soil Sci. Soc. Am. J. 81, 1257–1269. https://doi.org/10.2136/sssaj2017.02.0058.

Food and Agriculture Organization of the United Nations (FAO), 2021. AquaCrop (Online) [9 Jan. 2021). http://www.fao.org/aquacrop/en/.

Gao, Y., Pu, S., Zheng, C., Yi, S., 2019. An improved method for the calculation of unsaturated–saturated water flow by coupling the FEM and FDM. Sci. Rep. 9, 14995. https://doi.org/10.1038/s41598-019-51405-4.

Garen, D.C., Moore, D.S., 2005. Curve number hydrology in water quality modeling: uses, abuses, and future directions. J. Am. Water Resour. Assoc. 41 (2), 377–388. https://doi.org/10.1111/j.1752-1688.2005.tb03742.x.

Guest, G., Kröbel, R., Grant, B., Smith, W., Sansoulet, J., Pattey, E., Desjardins, R., Jego, G., Tremblay, N., Tremblay, G., 2017. Model comparison of soil processes in eastern Canada using DayCent, DNDC and STICS. Nutr. Cycl. Agroecosyst. 109 (3), 211–232. https://doi.org/10.1007/s10705-017-9880-8.

Guest, G., Smith, W., Grant, B., McConkey, B., Chipanshi, A., Reid, K., Kroebel, R., Martel, M., Desjardins, R., VanderZaag, A., Pattey, E., Glenn, A., Wilson, H., Balde, H., Wagner-Riddle, C., Drury, C.F., Fuller, K., Hayashi, M., Reynolds, D., 2018. Comparing the performance of the DNDC, Holos and VSMB models for predicting the water partitioning of various crops and sites across Canada. Can. J. Soil Sci. 98 (2), 212–231. https://doi.org/10.1139/cjss-2017-0112.

Hargreaves, G.H., Samani, Z.A., 1985. Reference crop evapotranspiration from temperature. Appl. Eng. Agric. 1, 96–99. https://doi.org/10.13031/2013.26773.

Hawkins, R.H., 1975. The importance of accurate curve numbers in the estimation of storm runoff. J. Am. Water Resour. Assoc. 11 (5), 887–890. https://doi.org/10.1111/j.1752-1688.1975.tb01810.x.

Hay, C.H., Irmak, S., 2009. Actual and reference evaporative losses and surface coefficients of a maize field during nongrowing (dormant) periods. J. Irrig. Drain. Eng. 135 (3), 313–322.

Hayashi, M., Jackson, J.F., Xu, L., 2010. Application of the Versatile Soil Moisture Budget model to estimate evaporation from prairie grassland. Can. Water Resour. J. 35 (2), 187–208. https://doi.org/10.4296/cwrj3502187.

Hayashi, M., Mohammed, G.A., Harrer, K., Farrow, C.R., 2012. Performance Evaluation and Improvement of the Versatile Soil Moisture Budget (VSMB) Model (Online) [05 Feb. 2021). https://www.parc.ca/rac/fileManagement/upload/Alberta%20AARDVersatile%20Soil%20Moisture%20Budget%20Model%20Feb2012.pdf.

He, Y., Hou, L., Wang, H., Hu, K., McConkey, B., 2014. A modelling approach to evaluate the long-term effect of soil texture on spring wheat productivity under a rain-fed condition. Sci. Rep. 4, 5736. https://doi.org/10.1038/srep05736.

Hishinuma, S., Takeuchi, K., Magome, J., 2014. Challenges of hydrological analysis for water resource development in semi-arid mountainous regions: case study in Iran. Hydrol. Sci. J. 59 (9), 1718–1737. https://doi.org/10.1080/02626667.2013.853879.

Islam, M.S., Claudio Paniconi, C., Putti, M., 2017. Numerical tests of the lookup table method in solving Richards' equation for infiltration and drainage in heterogeneous soils. Hydrology 4 (3), 33. https://doi.org/10.3390/hydrology4030033.

Joint Research Centre, 2021. PRZM_SW (Online) [6 Feb. 2021). https://esdac.jrc.ec.europa.eu/projects/przmsw#:~:text=PRZM%20(Pesticide%20Root%20Zone%20Model,1984)%20has%20been%20continuously%20improved.

Kondo, J., Yamazaki, T., 1990. A prediction model for snowmelt, snow surface temperature and freezing depth using a heat balance method. J. Appl. Meteorol. Climatol. 29, 375–384. https://doi.org/10.1175/1520-0450(1990)029%3C0375:APMFSS%3E2.0.CO;2.

Kowalik, T., Walega, A., 2015. Estimation of CN parameter for small agricultural watersheds using asymptotic functions. Water 7, 939–955. https://doi.org/10.3390/w7030939.

Lal, M., Mishra, S.K., Pandey, A., Pandey, R.P., Meena, P.K., Chaudhary, A., Jha, R.K., Shreevastava, A.K., Kumar, Y., 2017. Evaluation of the soil conservation service curve number methodology using data from agricultural plots. Hydrogeol. J. 25 (1), 151–167. https://doi.org/10.1007/s10040-016-1460-5.

Ling, L., Yusop, Z., 2014. A micro focus with macro impact: exploration of initial abstraction coefficient ratio (λ) in soil conservation curve number (CN) methodology. IOP Conf. Ser.: Earth Environ. Sci. 18, 012121. https://doi.org/10.1088/1755-1315/18/1/012121.

Makkink, G.F., 1957. Testing the Penman formula by means of lysimeters. J. Inst. Water Eng. 11, 277–288.
Malago, A., Pagliero, L., Bouraoui, F., Franchini, M., 2015. Comparing calibrated parameter sets of the SWAT model for the Scandinavian and Iberian peninsulas. Hydrol. Sci. J. 60 (5), 949–967. https://doi.org/10.1080/02626667.2014.978332.
Mante, A.A., Ranjan, R.S., 2017. HYDRUS (2d/3d) simulation of water flow through sandy loam soil under potato cultivation in southern Manitoba. Can. Biosyst. Eng. 59, 1.9–1.19. https://doi.org/10.7451/CBE.2017.59.1.9.
Mapes, K.L., Pricope, N.G., 2020. Evaluating SWAT model performance for runoff, percolation, and sediment loss estimation in low-gradient watersheds of the Atlantic coastal plain. Hydrology 7, 21. https://doi.org/10.3390/hydrology7020021.
Marek, G.W., Gowda, P., Evett, S.R., Baumhardt, R.L., Brauer, D.K., Howell, T.A., Marek, T.H., Srininvasan, R., 2016. Estimating evapotranspiration for dryland cropping systems in the semiarid Texas High Plains using SWAT. J. Am. Water Resour. Assoc. 52 (2), 298–314. https://doi.org/10.1111/1752-1688.12383.
Martel, M., Glenn, A., Wilson, H., Kröbel, R., 2018. Simulation of actual evapotranspiration from agricultural landscapes in the Canadian Prairies. J. Hydrol.: Reg. Stud. 15, 105–118. https://doi.org/10.1016/j.ejrh.2017.11.010.
Massmann, C., 2019. Modelling snowmelt in ungauged catchments. Water 11 (2), 301. https://doi.org/10.3390/w11020301.
Melaku, N.D., Wang, J., 2019. A modified SWAT module for estimating groundwater table at Lethbridge and Barons, Alberta, Canada. J. Hydrol. 575, 420–431. https://doi.org/10.1016/j.jhydrol.2019.05.052.
National Research Institute for Agriculture, Food and Environment (INRAE), 2020. Stics Model Overview (Online) [6 Jan 2021). https://www6.paca.inrae.fr/stics_eng/About-us/Stics-model-overview.
Neitsch, S.L., Arnold, J.G., Kiniry, J.R., Williams, J.R., 2011. Soil and Water Assessment Tool theoretical documentation version 2009. Texas Water Resources Institute Technical Report No. 406. Texas A&M University System.
Nyiraneza, J., Peters, R.D., Rodd, A.V., Grimmett, M.G., Jiang, Y., 2015. Improving productivity of managed potato cropping systems in eastern Canada: crop rotation and nitrogen source effects. Agron. J. 107 (4), 1447–1457. https://doi.org/10.2134/agronj14.0430.
PC-Progress, 2019. Hydrus (Online] [6 Jan. 2021). https://www.pc-progress.com/en/Default.aspx.
Perez-Sanchez, J., Senent-Aparicio, J., Segura-Mendez, F., Pulido-Velazquez, D., Srinivasan, R., 2019. Evaluating hydrological models for deriving water resources in peninsular Spain. Sustainability 11, 2872. https://doi.org/10.3390/su11102872.
Ponce, V.M., Hawkins, R.H., 1996. Runoff curve number: has it reached maturity? J. Hydrol. Eng. 1 (1), 11–19. https://doi.org/10.1061/(ASCE)1084-0699(1996)1:1(11).
Raes, D., Geerts, S., Kipkorir, E., Wellens, J., Sahli, A., 2006. Simulation of yield decline as a result of water stress with a robust soil water balance model. Agric. Water Manag. 81, 335–357. https://doi.org/10.1016/j.agwat.2005.04.006.
Raes, D., Steduto, P., Hsiao, T.C., Fereres, E., 2012. AquaCrop Version 4.0 - Calculation Procedures. Food and Agriculture Organization (FAO), Rome, Italy.
Ritter, A., Muñoz-Carpena, R., 2013. Performance evaluation of hydrological models: statistical significance for reducing subjectivity in goodness-of-fit assessments. J. Hydrol. 480, 33–45. https://doi.org/10.1016/j.jhydrol.2012.12.004.
Saltelli, A., Ratto, M., Andres, T., Campolongo, F., Cariboni, J., Gatelli, D., Saisana, M., Tarantola, S., 2008. Global Sensitivity Analysis. The Primer. John Wiley & Sons Ltd, England.
Saxton, K.E., Rawls, W.J., 2006. Soil water characteristic estimates by texture and organic matter for hydrologic solutions. Soil Sci. Soc. Am. J. 70, 1569–1578. https://doi.org/10.2136/sssaj2005.0117.
Scheider, W.A., Logan, L.A., Goebel, M.G., 1983. A comparison of two models to predict snowmelt in Muskoka-Haliburton, Ontario. In: Proc. 40th Annual Eastern Snow Conference. Toronto, Ontario, Canada, pp. 157–168.
Smith, W., Qi, Z., Grant, B., VanderZaag, A., Desjardins, R., 2019. Comparing hydrological frameworks for simulating crop biomass, water and nitrogen dynamics in a tile drained soybean-corn system: cascade vs computational approach. J. Hydrol. X 2, 100015. https://doi.org/10.1016/j.hydroa.2018.100015.
Smith, W., Grant, B., Qi, Z., He, W., VanderZaag, A., Drury, C., Helmers, M., 2020. Development of the DNDC model to improve soil hydrology and incorporate mechanistic tile drainage: a comparative analysis with RZWQM2. Environ. Model. Softw. 123, 104577. https://doi.org/10.1016/j.envsoft.2019.104577.
Snyder, R.L., Orang, M., Matyac, S., Eching, S., 2007. Crop Coefficients (Online] [6 Feb. 2021). http://biomet.ucdavis.edu/Evapotranspiration/CropCoef/Kc.pdf.
Soomro, A.G., Babar, M.M., Memon, A., Zaidi, A.Z., Ashraf, A., Lund, J., 2019. Sensitivity of direct runoff to curve number using the SCS-CN method. Civ. Eng. Urban Plan. Int. J. 5 (12), 2738–2746. https://doi.org/10.28991/cej-2019-03091445.
Suarez, L.A., 2005. PRZM-3, A Model for Predicting Pesticide and Nitrogen Fate in the Crop Root and Unsaturated Soil Zones: User's Manual for Release 3.12.2. EPA/600/R-05/111 (NTIS PB2006-101105). U.S. Environmental Protection Agency, Washington, DC.
Tafteh, A., Sepaskhah, A.R., 2012. Application of HYDRUS-1D model for simulating water and nitrate leaching from continuous and alternate furrow irrigated rapeseed and maize fields. Agric. Water Manag. 113, 19–29. https://doi.org/10.1016/j.agwat.2012.06.011.
Tedela, N.H., McCutcheon, S.C., Rasmussen, T.C., Hawkins, R.H., Swank, W.T., Campbell, J.L., Adams, M.B., Jackson, C.R., Tollner, E.W., 2012. Runoff curve numbers for 10 small forested watersheds in the mountains of the eastern United States. J. Hydrol. Eng. 17, 1188–1198. https://doi.org/10.1061/(ASCE)HE.1943-5584.0000436.
Texas A&M University, 2021. SWAT - Soil and Water Assessment Tool (online] [6 Feb. 2021). https://swat.tamu.edu/.
United States Department of Agriculture (USDA), 2021. National Engineering Handbook Hydrology Chapters (Online] [6 Jan. 2021). Natural Resources Conservation Service. https://www.nrcs.usda.gov/wps/portal/nrcs/detailfull/national/water/manage/hydrology/?cid=stelprdb1043063.
University of New Hampshire, 2021. The DNDC Model (Online] [6 Jan. 2021]. https://www.dndc.sr.unh.edu/.
USDA, 2004. Part 630 Hydrology National Engineering Handbook Chapter 11 Snowmelt (Online] [6 Jan. 2021]. https://directives.sc.egov.usda.gov/OpenNonWebContent.aspx?content=17753.wba.
USDA, 2020. RZWQM - Root Zone Water Quality Model (Online] [6 Jan. 2021]. https://www.ars.usda.gov/plains-area/fortcollins-co/center-for-agricultural-resources-research/rangeland-resources-systems-research/docs/system/rzwqm/.
Walega, A., Ksiazek, L., 2016. Influence of rainfall data on the uncertainty of flood simulation. Soil & Water Res. 11 (4), 277–284. https://doi.org/10.17221/156/2015-SWR.
Walega, A., Salata, T., 2019. Influence of land cover data sources on estimation of direct runoff according to SCS-CN and modified SME methods. Catena 172, 232–242. https://doi.org/10.1016/j.catena.2018.08.032.
Wang, E., Engel, T., 1998. Simulation of phenological development of wheat crops. Agric. Syst. 58 (1), 1–24. https://doi.org/10.1016/S0308-521X(98)00028-6.
Wang, E., Robertson, M.J., Hammer, G.L., Carberry, P.S., Holzworth, D., Meinke, H., Chapman, S.C., Hargreaves, J.N.G., Huth, N.I., McLean, G., 2002. Development of a generic crop model template in the cropping system model APSIM. Eur. J. Agron. 18 (1–2), 121–140. https://doi.org/10.1016/S1161-0301(02)00100-4.
Wang, H., Flerchinger, G.N., Lemke, R., Brandt, K., Goddard, T., Sprout, C., 2010. Improving SHAW long-term soil moisture prediction for continuous wheat rotations, Alberta, Canada. Can. J. Soil Sci. 90, 37–53. https://doi.org/10.4141/CJSS08084.
Wilson, H., Elliott, J., Macrae, M., Glenn, A., 2019. Near-surface soils as a source of phosphorus in snowmelt runoff from cropland. J. Environ. Qual. 48 (4), 921–930. https://doi.org/10.2134/jeq2019.04.0155.
Xiong, L., Wan, M., Wei, X., O'connor, K.M., 2009. Indices for assessing the prediction bounds of hydrological models and application by generalised likelihood uncertainty estimation / Indices pour évaluer les bornes de prévision de modèles hydrologiques et mise en oeuvre pour une estimation d'incertitude par vraisemblance généralisée. Hydrol. Sci. J. 54 (5), 852–871. https://doi.org/10.1623/hysj.54.5.852.
Zebarth, B.J., Danielescu, S., Nyiraneza, J., Ryan, M.C., Jiang, Y., Grimmett, M., Burton, D.L., 2015. Controls on nitrate loading and implications for BMPs under intensive potato production systems in Prince Edward Island. Canada. Groundw. Monit. Rem. 35, 30–42. https://doi.org/10.1111/gwmr.12088.
Zhu, H., Liu, T., Xue, B., Yinglan, A., Wang, G., 2018. Modified Richards' equation to improve estimates of soil moisture in two-layered soils after infiltration. Water 10, 1174. https://doi.org/10.3390/w10091174.